Pulse propagation through a slab with time-periodic dielectric function $\varepsilon(t)$

Jorge R. Zurita-Sánchez, J. H. Abundis-Patiño, and P. Halevi*

Instituto Nacional de Astrofísica, Óptica y Electrónica,
Apdo. Postal 51 y 216, Puebla, Pue. 72000, Mexico

**halevi@inaoep.mx*

Abstract: We describe pulse propagation through a slab with periodic dielectric function $\varepsilon(t)$, thus extending our previous investigation for monochromatic incidence [Phys. Rev. A **79**, 053821 (2009)]. Based on the concepts of phase and group delays, we prove that, for an incident quasi-monochromatic pulse, the transmitted pulse can be expressed as a superposition of partial pulses that are exact replicas of the incident pulse and that exit the slab with a time delay. These partial pulses have harmonic carrier frequencies $\omega_c - n\Omega$ (n is an integer, ω_c is the carrier frequency of the incident pulse, and $\Omega = 2\pi/T$ is the slab modulation frequency). We find numerically that these partial pulses can be fast (peak velocity $v_n > c$ or $v_n < 0$) or slow ($v_n \ll c$). Further, we investigate the peak velocity v_p of the outcoming pulse for several cases. We find that this peak velocity v_p and the partial peak velocities v_n do not diverge —as occurs to the group velocity v_g of the bulk dynamic-periodic medium when $\omega_c = \Omega/2$. We expect that these results could be verified in the microwave regime [see Halevi et al., Proc. SPIE **8095**, 80950I (2011)].

OCIS codes: (350.5500) Propagation; (130.7405) Wavelength conversion devices; (160.3918) Metamaterials.

References and links

1. C. G. B. Garrett and D. E. McCumber, "Propagation of a gaussian light pulse through an anomalous dispersion medium," Phys. Rev. A **1**, 305–313 (1970).
2. S. Chu and S. Wong, "Linear pulse propagation in an absorbing medium," Phys. Rev. Lett. **48**, 738–741 (1982).
3. S. P. Tewari and G. S. Agarwal, "Control of phase matching and nonlinear generation in dense media by resonant fields," Phys. Rev. Lett. **56**, 1811–1814 (1986).
4. S. E. Harris, J. E. Field, and A. Imamoğlu, "Nonlinear optical processes using electromagnetically induced transparency," Phys. Rev. Lett. **64**, 1107–1110 (1990).
5. M. Xiao, Y. Li, S. Jin, and J. Gea-Banacloche, "Measurement of dispersive properties of electromagnetically induced transparency in rubidium atoms," Phys. Rev. Lett. **74**, 666–669 (1995).
6. L. V. Hau, S. E. Harris, Z. Dutton, and C. H. Behroozi, "Light speed reduction to 17 meters per second in an ultracold atomic gas," Nature **397**, 594–598 (1999).
7. L. J. Wang, A. Kuzmich, and A. Dogariu, "Gain-assisted superluminal light propagation," Nature **406**, 277–279 (2000).
8. A. Dogariu, A. Kuzmich, H. Cao, and L. J. Wang, "Superluminal light pulse propagation via rephasing in a transparent anomalously dispersive medium," Opt. Express **8**, 344–350 (2001).
9. M. S. Bigelow, N. N. Lepeshkin, and R. W. Boyd, "Observation of ultraslow light propagation in a ruby crystal at room temperature," Phys. Rev. Lett. **90**, 113903 (2003).
10. K. Y. Song, M. G. Herráez, and L. Thévenaz, "Observation of pulse delaying and advancement in optical fibers using stimulated brillouin scattering," Opt. Express **13**, 82–88 (2005).
11. R. W. Boyd and D. J. Gauthier, "Slow and Fast Light," in *Progress in Optics*, Vol. 43, E. Wolf, ed. (Elsevier, Amsterdam, 2002), pp. 497–530.

#159929 - $15.00 USD Received 14 Dec 2011; revised 19 Jan 2012; accepted 26 Jan 2012; published 22 Feb 2012

12. J. R. Zurita-Sánchez, P. Halevi, and J. C. Cervantes-González, "Reflection and transmission of a wave incident on a slab with a time-periodic dielectric function $\varepsilon(t)$," Phys. Rev. A **79**, 053821 (2009).
13. J. R. Zurita-Sánchez and P. Halevi, "Resonances in the optical response of a slab with time-periodic dielectric function $\varepsilon(t)$," Phys. Rev. A **81**, 053834 (2010).
14. F. Biancalana, A. Amann, A. V. Uskov, and E. P. O'Reilly, "Dynamics of light propagation in spatiotemporal dielectric structures," Phys. Rev. E **75**, 046607 (2007).
15. Y. Xiao, G. P. Agrawal, and D. N. Maywar, "Spectral and temporal changes of optical pulses propagating through time-varying linear media," Opt. Lett. **36**, 505–507 (2011).
16. S. F. Preble, Q. Xu, and M. Lipson, "Changing the colour of light in a silicon resonator," Nat. Photonics **1**, 293–296 (2007).
17. M. W. McCutcheon, A. G. Pattantyus-Abraham, G. W. Rieger, and J. F. Young, "Emission spectrum of electromagnetic energy stored in a dynamically perturbed optical microcavity," Opt. Express **15**, 11472–11480 (2007).
18. T. Tanabe, M. Notomi, H. Taniyama, and E. Kuramochi, "Dynamic release of trapped light from an ultrahigh-q nanocavity via adiabatic frequency tuning," Phys. Rev. Lett. **102**, 043907 (2009).
19. T. Kampfrath, D. M. Beggs, T. P. White, A. Melloni, T. F. Krauss, and L. Kuipers, "Ultrafast adiabatic manipulation of slow light in a photonic crystal," Phys. Rev. A **81**, 043837 (2010).
20. W. J. Padilla, A. J. Taylor, C. Highstrete, M. Lee, and R. D. Averitt, "Dynamical electric and magnetic metamaterial response at terahertz frequencies," Phys. Rev. Lett. **96**, 107401 (2006).
21. V. J. Logeeswaran, A. N. Stameroff, M. S. Islam, W. Wu, A. M. Bratkovsky, P. J. Kuekes, S. Y. Wang, and R. S. Williams, "Switching between positive and negative permeability by photoconductive coupling for modulation of electromagnetic radiation," Appl. Phys. A **87**, 209–216 (2007).
22. E. Poutrina, S. Larouche, and D. R. Smith, "Parametric oscillator based on a single-layer resonant metamaterial," Opt. Comm. **283**, 1640–1646 (2010).
23. A. R. Katko, S. Gu, J. P. Barret, B.-I. Popa, G. Shvets, and S. A. Cummer, "Phase conjugation and negative refraction using nonlinear active metamaterials," Phys. Rev. Lett. **105**, 123905 (2010).
24. P. Halevi, U. Algredo-Badillo, and J. R. Zurita-Sánchez, "Optical response of a slab with time-periodic dielectric function $\varepsilon(t)$: towards a dynamic metamaterial," in *Active Photonic Materials IV*, G. S. Subramania and S. Foteinopoulou, eds., Proc. SPIE **8095**, 80950I (2011).
25. A. Papoulis, *Signal Analysis* (McGraw-Hill, Tokio, 1977).
26. P. Halevi, "Transit velocity of a pulse through a transparent plate," Opt. Lett. **11**, 759–760 (1986).
27. P. Halevi and L. D. Valenzuela, "Propagation of a broad light pulse through a plate," J. Opt. Soc. Am. B **8**, 1512–1515 (1991).

1. Introduction

Over the past two decades, a high degree of control of pulse velocity in various media has been accomplished experimentally. Diverse experimental schemes lead to both slow light ($v_g \ll c$) and fast light (either $v_g > c$ or $v_g < 0$) [c is the vacuum light velocity and v_g is the group velocity]. Originally, Garrett and McCumber theoretically predicted that, in the vicinity of an absorption line, the peak velocity of a Gaussian pulse is equal to the group velocity even if $v_g > c$, $v_g = \infty$, or $v_g < 0$ [1]. Later, this prediction was confirmed experimentally by Chu and Wong [2]. Subsequent studies found that the interaction of a gas of atoms with a strong field could eliminate the absorption and modify the dispersive refractive index seen by a weak-intensity wave [3–5]. This possibility was the milestone for achieving great pulse velocity control. For example, in an ultracold gas of atoms a very low group velocity [$v_g \approx c/(1.76 \times 10^7)$] was measured [6], while in a hot gas of caesium atoms, fast light was observed $v_g \approx -c/310$ [7] where this superluminal velocity in a medium with anomalous dispersion is simply explained by light interference [8]. Other nonlinear mechanisms, as the coherent population oscillations and stimulated Brillouin scattering, allow to observe the slow-fast light effects in solid media as ruby [9] and in optical fibers [10]. Since solids are propitious for practical implementation, potential applications in optical communications such as pulse delay control devices have been envisioned. Despite these remarkable achievements, a central concern still is pulse propagation without distortion (that is inexorably caused by the dispersion of the medium) [11].

Recently, there is renewed interest in exploring dynamic media that could lead to new methods for controlling and manipulating light propagation. The readers can find numerous references on dynamic media in our recent works [12, 13]. We mention that, in the context of pulse

#159929 - $15.00 USD Received 14 Dec 2011; revised 19 Jan 2012; accepted 26 Jan 2012; published 22 Feb 2012

propagation, it was found theoretically that a pulse passing through layered dielectric structures with arbitrary space-time dependence of the refractive index experiences reshaping (compression and broadening) and its central frequency is shifted [14]. Similar effects are reported for pulses propagating in a linear medium with time-varying refractive index [15]. Spectral shifts of pulses, resulting from the passage through dynamic cavities and waveguides, were observed [16–19]. In other recent studies, the incorporation of dynamic inclusions has been explored. Dynamic metamaterials that work at GHz and THz frequencies can be made by filling the split-ring resonator gaps with a photoconductive semiconductor [20, 21]. These dynamic metamaterials could exhibit an effective dielectric function that can be strongly modulated with a frequency ~ 1 GHz (limited by the lifetime and the mobility of the charge carriers). The parametric response in a single split-ring resonator with a time-varying capacitive element was studied in [22]. Phase conjugation and negative refraction effects can occur in a metamaterial composed of split-ring resonators with nonlinear varactors [23].

In prior studies, we theoretically analyzed the wave propagation in a medium whose dielectric function $\varepsilon(t)$ varies periodically in time, namely, $\varepsilon(t) = \varepsilon(t+T)$ (T is the period). We found that the dispersion relation is a band structure with forbidden *wave vector* gaps and we studied the electromagnetic response of a dynamic-periodic slab to monochromatic plane wave excitation [12]. Due to the periodic modulation, harmonics $\omega - n\Omega$ are generated (ω is the angular frequency of the exciting monochromatic wave, $\Omega = 2\pi/T$ is the modulation frequency, n is an integer). Consequently, the slab becomes a polychromatic source. Later, we found that this dynamic-periodic slab can exhibit resonances when the excitation frequency is $\omega = m\Omega/2$ with $m = 1,3,5,\ldots$ and, in addition, the modulating frequency obeys a certain condition [13]. On the other hand, the temporal variation of our dielectric function relies on the interaction of an external agent with the medium. For optical frequencies, the modulation strength of the dielectric function that can be reached by current nonlinear methods is a small fraction of the unperturbed dielectric constant, and the typical temporal response of a material allows modulating frequencies not higher than ~ 10 GHz. On the other hand, very recently we have shown that, in the long-wavelength limit, a low-pass dynamic transmission line for microwaves can be characterized by a time-dependent effective dielectric function $\varepsilon_{\text{ef}}(t)$ with a large modulation strength, thus overcoming the aforementioned limitation for optical frequencies [24]. This transmission line is a linear array of cells that are formed each by an inductance L and a varactor whose capacitance $C(t)$ is modulated periodically. The response of this transmission line can be characterized with an effective dielectric function $\varepsilon_{\text{ef}}(t) = C(t)/(\varepsilon_o a)$ (a is the lattice constant and ε_o is the vacuum permittivity) with the restriction that the dominant wavevectors k satisfy $ka \ll 1$. Therefore, the experimental implementation of a medium exhibiting an effective and strongly modulated dielectric function $\varepsilon(t)$ is feasible, at least in the microwave regime.

We focus on the transmission of a pulse through a slab whose dielectric function $\varepsilon(t)$ varies periodically, namely, $\varepsilon(t) = \varepsilon(t+T)$ (T is the period). We present a theoretical framework for obtaining the transmitted and reflected pulses when a pulse is incident on this dynamic-periodic slab. This framework is an extension of our aforementioned theory of bulk dynamic-periodic media and response of a dynamic slab excited by a monochromatic plane wave [12]. Furthermore, we present an alternative description of the transmitted pulses for an incident *quasi-monochromatic* pulse that is based on the concepts of group and phase delays [25]. From this description, the transmitted pulse can be decomposed as the superposition of partial pulses. Particularly, we analyze the pulse propagation through the dynamic-periodic slab for incident Gaussian pulses with narrow (quasi-monochromatic) and with broad bandwidths for selected values of the carrier frequency, slab thickness, and modulation strength. We investigate the propagation velocities of the aforementioned partial pulses for incoming quasi-monochromatic pulses. Also, we study the peak velocity of the pulse when a Gaussian pulse is incident on

#159929 - $15.00 USD Received 14 Dec 2011; revised 19 Jan 2012; accepted 26 Jan 2012; published 22 Feb 2012

the slab. We address the question whether these propagation velocities are related to the group velocity obtained from the bulk dispersion relation. We pay special attention to the case when the carrier frequency of the incoming pulse is $\omega_c = n\Omega/2$, since the dispersion relation (a band structure with forbidden wave vector gaps) yields infinite group velocities at these frequencies. Finally, we discuss the energy balance between the incident pulse and the outcoming transmitted and reflected pulses.

This paper is organized as follows. Section 2 presents the general theory of pulse propagation through the dynamic-periodic slab (reflected and transmitted pulses). In addition, we present a simplified description of the transmitted pulses that is based on the concepts of phase and group delays, being valid for quasi-monochromatic incident pulses. In Sec. 3, we analyze the pulse propagation of quasi-monochromatic incident Gaussian pulses for particular carrier frequencies, slab thicknesses, and modulation strengths. Conversely, Sec. 4 deals with the analysis of the pulse transmission of a Gaussian pulse with large spectral bandwidth. Investigation of the peak velocity of a pulse propagating through the dynamic slab is presented in Sec. 5. Section 6 is devoted to the discussion of the energy carried by the reflected and transmitted pulses in comparison with that of the incoming pulse. Section 7 contains the conclusions.

2. Theory

2.1. An electromagnetic pulse interacting with a dynamic slab

In Ref. [12] we studied a dynamic medium whose dielectric function $\varepsilon(t)$ varies periodically with the time t, the period T being related to the modulation frequency Ω by $T = 2\pi/\Omega$. For an excitation frequency ω, the modulation induces an infinite number of harmonics with frequencies $\omega - n\Omega$, $n = 0, \pm 1, \pm 2, \ldots$ Moreover, for any given ω and a given propagation direction (say, y), an infinite number of plane waves, differing in their wavelengths, can propagate. These are characterized by wave vectors $k_p(\omega)$, $p = 1, 2, \ldots$ The index p labels the wavevector bands, and the corresponding band structure is characterized by band gaps Δk between adjacent bands p and $p+1$. We also showed in Ref. [12] that a monochromatic wave (frequency ω), normally incident at a slab of thickness D in vacuum, gives rise to reflected and transmitted waves with all the frequencies $\omega - n\Omega$ (all integers n). Furthermore, inside the slab, in addition to waves with wave vectors $k_p(\omega)$ there will also be excited counterpropagating waves with wave vectors $-k_p(\omega)$. Here we apply the former treatment to an incident pulse or wave packet whose electric field is given by

$$E_i(y,t) = \int_{-\infty}^{\infty} E_o(\omega) \exp[i\omega(y/c - t)] \mathrm{d}\omega, \tag{1}$$

where c is the vacuum speed of light. The spectral amplitude $E_o(\omega)$ is given by the inverse transform

$$E_o(\omega) = \frac{1}{2\pi} \int_{-\infty}^{\infty} E_i(0,t) \exp(i\omega t) \mathrm{d}\omega. \tag{2}$$

It is now straightforward to generalize the Eqs. (34), (36), and (38) of Ref. [12] for, respectively, the electric field within the slab E_s, the reflected field E_r, and the transmitted field E_t:

$$\begin{aligned} E_s(y,t) &= \sum_{p=1}^{\infty} \sum_{n=-\infty}^{\infty} \int_{-\infty}^{\infty} \left\{ A_p(\omega) \exp[ik_p(\omega)y] + B_p(\omega) \exp[-ik_p(\omega)y] \right\} \\ &\quad \times e_{pn}(\omega) \exp[-i(\omega - n\Omega)t] \mathrm{d}\omega, \end{aligned} \tag{3}$$

$$E_r(y,t) = \sum_{n=-\infty}^{\infty} \int_{-\infty}^{\infty} E_n^r(\omega) \exp[-i(\omega - n\Omega)(y/c + t)] \mathrm{d}\omega, \tag{4}$$

$$E_t(y,t) = \sum_{n=-\infty}^{\infty} \int_{-\infty}^{\infty} E_n^t(\omega) \exp\{i(\omega - n\Omega)[(y-D)/c - t]\} \mathrm{d}\omega. \tag{5}$$

#159929 - $15.00 USD Received 14 Dec 2011; revised 19 Jan 2012; accepted 26 Jan 2012; published 22 Feb 2012

Here, $e_{pn}(\omega)$ is the amplitude of the bulk mode of wave vector k_p and harmonic $\omega - n\Omega$, while $A_p(\omega)$ and $B_p(\omega)$ are the spectral amplitudes of the waves propagating, respectively, to the right and left in the slab. In Eqs. (4) and (5), $E_n^{\rm r}(\omega)$ and $E_n^{\rm t}(\omega)$ are the spectral amplitudes of the reflected and transmitted fields, respectively. For a given $E_{\rm o}(\omega)$, the amplitudes $A_p(\omega)$, $B_p(\omega)$, $E_n^{\rm r}(\omega)$, and $E_n^{\rm t}(\omega)$ are determined from the linear set of equations (45)-(48) of Ref. [12], obtained from the boundary conditions for the electric and magnetic fields at the interfaces $y = 0$ and $y = D$.

Our analysis of the reflected and transmitted pulses will take place at the slab borders $y = 0,$ and D, respectively. Then, from the Eqs. (4) and (5) we obtain

$$E_{\rm r}(0,t) = \sum_{n=-\infty}^{\infty} \int_{-\infty}^{\infty} r_n(\omega) E_{\rm o}(\omega) \exp[-i(\omega - n\Omega)t] {\rm d}\omega, \tag{6}$$

$$E_{\rm t}(D,t) = \sum_{n=-\infty}^{\infty} \int_{-\infty}^{\infty} t_n(\omega) E_{\rm o}(\omega) \exp[-i(\omega - n\Omega)t] {\rm d}\omega, \tag{7}$$

where $r_n(\omega) \equiv E_n^{\rm r}(\omega)/E_{\rm o}(\omega)$ and $t_n(\omega) \equiv E_n^{\rm t}(\omega)/E_{\rm o}(\omega)$ are the reflection and transmission coefficients for the harmonic $\omega - n\Omega$, respectively.

2.2. Quasi-monochromatic pulses

We analyze the response to an incident quasi-monochromatic pulse. This incident pulse is represented as the product of a slow time-varying signal $\mathscr{E}(t)$ peaked at $t = 0$ and a harmonic signal oscillating with frequency $\omega_{\rm c}$ (carrier frequency), that is,

$$E_{\rm i}(y = 0, t) = \mathscr{E}(t) \exp(-i\omega_{\rm c} t). \tag{8}$$

By performing the variable transformation $\omega = \omega_{\rm c} + \alpha$, Eq. (2) for $E_{\rm o}(\omega)$ yields

$$E_{\rm o}(\alpha + \omega_{\rm c}) = \tilde{\mathscr{E}}(\alpha), \tag{9}$$

where $\tilde{\mathscr{E}}(\alpha)$ is the Fourier transform of $\mathscr{E}(t)$, namely,

$$\tilde{\mathscr{E}}(\alpha) = \frac{1}{2\pi} \int_{-\infty}^{\infty} \mathscr{E}(t) \exp(i\alpha t) {\rm d}t. \tag{10}$$

By also carrying out the transformation $\omega = \alpha + \omega_{\rm c}$ to Eq. (7) and using Eq. (9), the transmitted pulse becomes

$$E_{\rm t}(y = D, t) = \sum_{n=-\infty}^{\infty} \exp[-i(\omega_{\rm c} - n\Omega)t] \int_{-\infty}^{\infty} t_n(\omega_{\rm c} + \alpha) \tilde{\mathscr{E}}(\alpha) \exp[-i\alpha t] {\rm d}\alpha. \tag{11}$$

We express $t_n(\omega)$ as

$$t_n(\omega) = A_n(\omega) \exp[i\phi_n(\omega)], \tag{12}$$

where $A_n(\omega) \equiv |t_n(\omega)|$ and $\phi_n(\omega) \equiv \arg[t_n(\omega)]$ ($\arg[\ldots]$ denotes argument). Since $\mathscr{E}(t)$ is a slowly time-varying signal, $\tilde{\mathscr{E}}(\alpha)$ is *sharply* localized around $\alpha = 0$, namely most spectral components of the pulse should satisfy the condition that

$$|\alpha| = |\omega - \omega_{\rm c}| \ll \omega_{\rm c}. \tag{13}$$

As a consequence, we can expand $t_n(\omega)$ in a power series around $\omega_{\rm c}$. The first order approximation renders

$$t_n(\omega_{\rm c} + \alpha) \approx A_n(\omega_{\rm c}) \exp[i\phi_n(\omega_{\rm c})] + \left[A_n'(\omega_{\rm c}) + i\phi_n'(\omega_{\rm c}) A_n(\omega_{\rm c})\right] \exp[i\phi_n(\omega_{\rm c})]\alpha. \tag{14}$$

#159929 - $15.00 USD Received 14 Dec 2011; revised 19 Jan 2012; accepted 26 Jan 2012; published 22 Feb 2012

Here, the superscript "$\prime$" denotes derivative. We further consider that the term containing $A_n'(\omega_c)$ can be neglected. This implies that

$$\left|\frac{A_n'(\omega_c)}{A_n(\omega_c)}\right| \ll \left|\phi_n'(\omega_c)\right|. \tag{15}$$

With this assumption and Eq. (12), the approximation (14) is reduced to

$$t_n(\omega_c+\alpha) \approx A_n(\omega_c)\exp[i\phi(\omega_c)]\left[1+i\phi_n'(\omega_c)\alpha\right] \approx t_n(\omega_c)\exp[i\phi_n'(\omega_c)\alpha]. \tag{16}$$

Hence, the transmitted pulse at the end of the slab becomes

$$\begin{aligned} E_t(y=D,t) &= \sum_{n=-\infty}^{\infty} A_n(\omega_c)\exp\{-i[(\omega_c-n\Omega)t-\phi_n(\omega_c)]\} \\ &\quad \times \int_{-\infty}^{\infty} \tilde{\mathscr{E}}(\alpha)\exp\{-i\alpha[t-\phi_n'(\omega_c)]\}\mathrm{d}\alpha, \\ &= \sum_{n=-\infty}^{\infty} t_n(\omega_c)\exp[-i(\omega_c-n\Omega)t]\mathscr{E}[t-\phi_n'(\omega_c)]. \end{aligned} \tag{17}$$

Then, the transmitted field can be described as a superposition of pulses that correspond to each of the harmonics created by the dynamic slab. The amplitude of n-th pulse is $A_n(\omega_c)$. Moreover, the partial carrier signals oscillate with frequencies $\omega_c - n\Omega$ and acquire phases $\phi_n(\omega_c)$ (*phase delays* [25]), whereas the pulse envelope shape remains unchanged, but suffers temporal shifts $\phi_n'(\omega_c)$ (*group delays* [25]). These outcoming pulses are characterized by the transmission coefficient $t_n(\omega_c)$.

Now let us consider as a temporal reference the time in which the peak of incident envelope hits the entrance interface. Since the envelope of the n-th outcoming partial pulse is just a delayed replica of the incident one, the peak of this partial pulse must exit the slab at a time $\phi_n'(\omega_c)$ after this reference. Therefore, the group delay of the partial pulses can be related to peak velocities as

$$v_n = D/\phi_n'(\omega_c). \tag{18}$$

3. Quasi-monochromatic Gaussian pulses

We apply the theory to the case of an incident Gaussian pulse having the form

$$E_i(y,t) = \exp[-(y-ct)^2/(c^2\tau^2)]\cos[\omega_c(y/c-t)], \tag{19}$$

where τ is the temporal width of the pulse and an unitary amplitude is assumed. The peak hits the left surface of the slab ($y=0$) at the time $t=0$. Equation (19) corresponds to the real part of Eq. (8), that is, $\mathscr{E}(t) = \exp(-t^2/\tau^2)$. The spectral amplitude of the Gaussian pulse yields [Eq. (2)]

$$E_o(\omega) = \frac{\tau}{4\sqrt{\pi}}\left\{\exp[-\tau^2(\omega-\omega_c)^2/4] + \exp[-\tau^2(\omega+\omega_c)^2/4]\right\}, \tag{20}$$

where the spectral width is $\Delta\omega = 2/\tau$. By Eq. (13), we assume that $\omega_c\tau \gg 1$.

We consider that the dielectric function $\varepsilon(t)$ of the slab is modulated sinusoidally as

$$\varepsilon(t) = \bar{\varepsilon}\left[1+M\sin(\Omega t)\right], \tag{21}$$

where $\bar{\varepsilon}$ is the time average of $\varepsilon(t)$, and M is the modulation strength. For reference to our previous work, we set $\bar{\varepsilon} = 5.25$ and, $M = 0.016$ ("weak modulation"), 0.162 ("moderate modulation") or 0.648 ("strong modulation"). In addition, it is convenient to normalize the modulation frequency as

$$\tilde{\Omega} = \Omega t_s = \Omega\sqrt{\bar{\varepsilon}}D/c \tag{22}$$

#159929 - $15.00 USD Received 14 Dec 2011; revised 19 Jan 2012; accepted 26 Jan 2012; published 22 Feb 2012

and the time as

$$\tilde{t} = t/t_s = tc/(\sqrt{\bar{\varepsilon}}D), \tag{23}$$

where t_s is the time it takes for the peak of a pulse propagating at speed $v_s = c/\sqrt{\bar{\varepsilon}}$ to cross the slab. Note that $\Omega t = \tilde{\Omega}\tilde{t}$.

We compare the numerical simulations for the transmitted pulse obtained from the exact response (5) and for the approximate response (17) for particular cases. First we consider that the normalized modulation frequency is $\tilde{\Omega} = 2$ and the incident pulse has a carrier frequency $\omega_c = \Omega/2$ and spectral width $\Delta\omega/\Omega = 0.1$. This pulse is shown in Fig. 1(a) as function of $\tilde{t}$. Figures 1(b) and 1(c) show the transmitted pulse arising from the exact (5) and the approximate (17) responses for the cases: $M = 0.162$ (moderate modulation) and 0.648 (strong modulation). Despite that $\Delta\omega$ is not very small in comparison with ω_c ($\omega_c\tau = 10$), we notice from Figs. 1(b) and 1(c) that practically perfect matches between the exact and the approximate responses are obtained. We also observe in these figures that the transmitted pulse for $M = 0.648$ is more distorted than for $M = 0.162$. This is explained by the fact that the amplitudes of the higher order harmonics generated inside the dynamic slab become larger as the modulation strength increases (see also [12]). Now we consider another particular case where $\omega_c/\Omega = 0.67$, $\Delta\omega/\Omega = 0.1$, $M = 0.648$, and $\tilde{\Omega} = 8$, that is, the carrier frequency ω_c and the normalized modulation frequency $\tilde{\Omega}$ have increased with respect to previous strong modulation

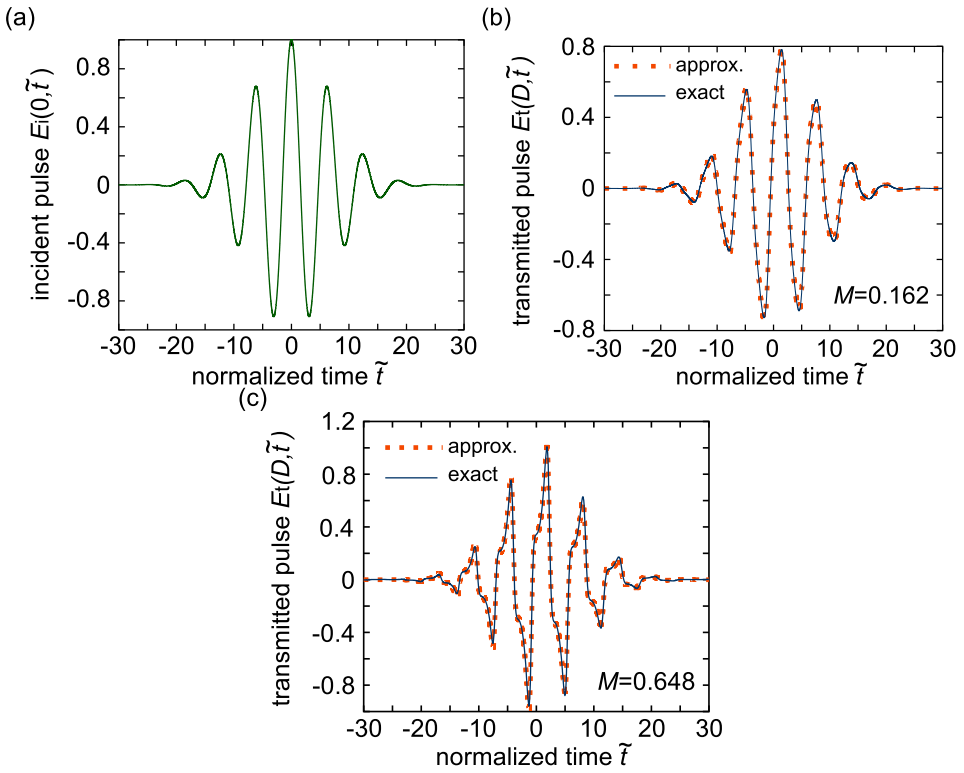

Fig. 1. Incident and transmitted pulses as a function of the normalized time $\tilde{t}$ for a slab with normalized modulation frequency $\tilde{\Omega} = 2$. (a) The incident electric pulse E_i with carrier frequency $\omega_c/\Omega = 0.5$ and spectral bandwidth $\Delta\omega/\Omega = 0.1$. (b) The transmitted pulse for a modulation strength $M = 0.162$. (c) The transmitted pulse for a modulation strength $M = 0.648$. Here $\omega_c\tau = 10$ and $t_s\Delta\omega = 0.2$.

#159929 - $15.00 USD Received 14 Dec 2011; revised 19 Jan 2012; accepted 26 Jan 2012; published 22 Feb 2012

case. The incident pulse is depicted in Fig. 2(a), while the transmitted pulse resulting from the exact and approximate responses is shown in Fig. 2(b). For this case, contrary to the prior cases,

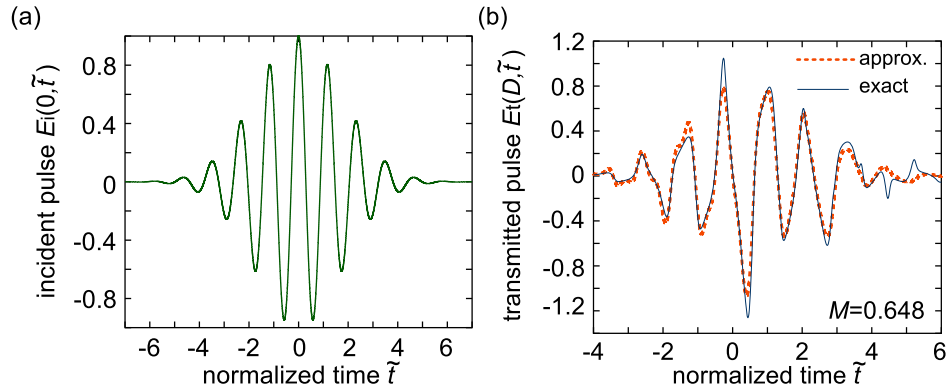

Fig. 2. Incident and transmitted pulses as a function of the normalized time $\tilde{t}$ for a slab with normalized modulation frequency $\tilde{\Omega} = 8$ and modulation strength $M = 0.648$. (a) The incident electric pulse E_i with carrier frequency $\omega_c/\Omega = 0.67$ and spectral bandwidth $\Delta\omega/\Omega = 0.1$. (b) The transmitted pulse. Here $\omega_c\tau = 13.4$ and $t_s\Delta\omega = 0.8$.

there is a difference between the exact and the approximate responses. This difference is more evident at times $\tilde{t} \approx -1.3$, -0.3, 0.4, 4.3 and 5.2. We attribute the deviation of the approximate response from the exact one to the fact that the condition $\tau \gg D/v_s = t_s$ (equivalently $t_s\Delta\omega \ll 2$) for obtaining a single well defined outcoming pulse is not satisfied as well as in Fig. 1(c). Now we reduce the pulse spectral width of the incident pulse one order of magnitude, that is, $\Delta\omega/\Omega = 0.01$. This is illustrated in Fig. 3(a). Due to this spectral reduction, the approx-

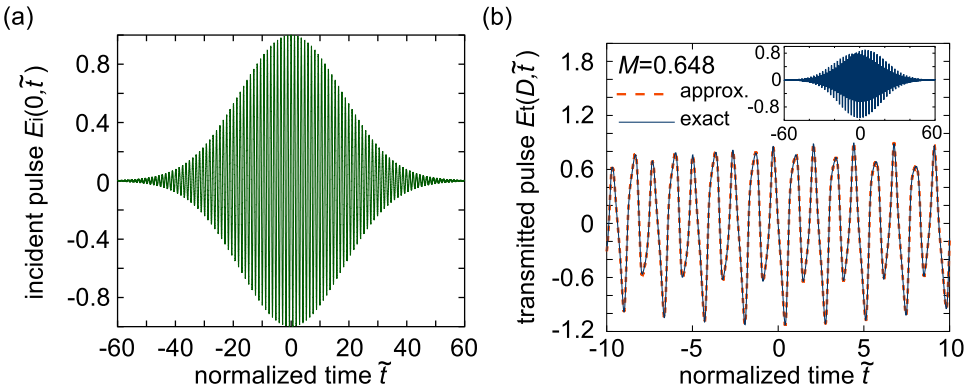

Fig. 3. Incident and transmitted pulses as a function of the normalized time $\tilde{t}$ for a slab with normalized modulation frequency $\tilde{\Omega} = 8$ and modulation strength $M = 0.648$. (a) The incident electric pulse E_i with carrier frequency $\omega_c/\Omega = 0.67$ and spectral bandwidth $\Delta\omega/\Omega = 0.01$. (b) The transmitted pulse (inset shows the whole pulse). Here $\omega_c\tau = 134$ and $t_s\Delta\omega = 0.08$.

imate and the exact responses coincide as seen in Fig. 3(b). Therefore, we have shown that the transmission of an incident *quasi-monochromatic* pulse passing through the dynamic-periodic slab can be well described by Eq. (17).

Now we discuss the implications resulting from the description based on the concepts of group and phase delays. According to Eq. (17), the transmitted pulse can be decomposed as a

#159929 - $15.00 USD Received 14 Dec 2011; revised 19 Jan 2012; accepted 26 Jan 2012; published 22 Feb 2012

superposition of exact replicas of the incident pulse in which the partial carrier signal has a frequency $\omega_c - n\Omega$ ($n = 0, \pm 1, \pm 2, \ldots$) and suffers a phase delay $\phi_n(\omega_c)$, the envelope experiences a time delay $\phi_n'(\omega_c)$, and the amplitude is $A_n(\omega_c)$. In terms of the normalized parameters $\tilde{t}$ and $\tilde{\Omega}$, the partial Gaussian pulse at the slab exit ($y = D$) for the harmonic n can be expressed as

$$E_n^t(D,\tilde{t}) = A_n(\hat{\omega}_c)\exp[-t_s^2(\tilde{t} - \Delta\tilde{\tau}_n)^2/\tau^2]\cos\left[(\hat{\omega}_c - n)\tilde{\Omega}\tilde{t} - \phi_n(\hat{\omega}_c)\right], \tag{24}$$

where $\hat{\omega}_c \equiv \omega_c/\Omega$ is the normalized carrier frequency and $\Delta\tilde{\tau}_n = (1/\tilde{\Omega})d\phi_n/d\hat{\omega}_c$ is the normalized temporal shift of the partial pulse. Tables 1 and 2 show the characterizing parameters of the partial pulses for the lowest orders in which the transmitted pulses of Figs. 1(c) and 3(b) are decomposed, respectively. From Tables 1 and 2, we notice that $\Delta\tilde{\tau}_n$ that can be either *positive or negative*.

Table 1. The characteristics of the outcoming partial Gaussian pulses [Eq. (24)] for the harmonic n and modulation strength $M = 0.648$ (strong). Incident Gaussian pulse with carrier frequency $\omega_c/\Omega = 0.5$ and spectral width $\Delta\omega/\Omega = 0.1$; slab with normalized modulation frequency $\tilde{\Omega} = 2$. Here $\omega_c\tau = 10$ and $t_s\Delta\omega = 0.2$.

n	$A_n(\hat{\omega}_c)$	$\phi_n(\hat{\omega}_c)/\pi$	$\Delta\tilde{\tau}_n$	v_n/c
-2	0.1213	-0.9132	0.2565	1.7013
-1	0.3457	-0.3268	0.6186	0.7055
0	0.16261	0.3315	0.8964	0.4869
1	0.1940	1.0000	1.1998	0.3637

Table 2. The characteristics of the outcoming partial Gaussian pulses [Eq. (24)] for the harmonic n and modulation strength $M = 0.648$ (strong). Incident Gaussian pulse with carrier frequency $\omega_c/\Omega = 0.67$ and spectral width $\Delta\omega/\Omega = 0.01$; slab with normalized modulation frequency $\tilde{\Omega} = 8$. Here $\omega_c\tau = 134$ and $t_s\Delta\omega = 0.08$.

n	$A_n(\hat{\omega}_c)$	$\phi_n(\hat{\omega}_c)/\pi$	$\Delta\tilde{\tau}_n$	v_n/c
-3	0.0064	0.6759	8.0334	0.0543
-2	0.0141	0.1372	-5.4397	-0.0802
-1	0.1460	0.16298	-0.4390	-0.9942
0	0.7907	-0.3944	0.5524	0.7901
1	0.1885	0.8299	1.2764	0.3419
2	0.0581	-0.4351	1.3903	0.3139

The transmission of partial pulses (for a given harmonic n) can be both fast and slow. On one hand, *fast pulse* propagation occurs when $\Delta\tilde{\tau}_n < 0$ or $0 < \Delta\tilde{\tau}_n < 1/\sqrt{\varepsilon} = 0.4364$ (corresponding to $\Delta t < D/c$), namely, when the transmitted pulse peak has emerged before the incident pulse peak has entered into the slab or when the transmitted pulse peak has traveled at a velocity faster than c, respectively. As seen in Table 1, fast light appears for the partial pulse $n = -2$ for which the peak velocity is $v_{-2}/c = 1.7013$. Also in Table 2, fast light shows up for the partial pulses with harmonics $n = -2, -1$. For these partial pulses, the temporal shifts are negative ($\Delta\tilde{\tau}_{-2} = -5.4397$ and $\Delta\tilde{\tau}_{-1} = -0.4390$) which yield negative peak velocities. This effect of the pulse peak propagating with velocity $v_n > c$ or $v_n < 0$ does not violate the causality principle, but comes from the interference of the generated spectral components inside the slab that causes the reconstruction of the partial pulses at advanced times.

On the other hand, *slow pulse* transmission happens when $\Delta\tilde{\tau}_n \gg 1/\sqrt{\varepsilon}$, that is, the transmitted pulse peak has traveled at a velocity much slower than c. In Table 2, we call attention

#159929 - $15.00 USD Received 14 Dec 2011; revised 19 Jan 2012; accepted 26 Jan 2012; published 22 Feb 2012

to the partial pulse $n=-3$ whose peak exits the slab with a long delay $\Delta\tilde{\tau}_{-3}=8.0334$ which corresponds to a peak velocity $v_{-3}/c=0.0543$. This peak velocity reduction is due to the same aforementioned interference effect, but the partial pulse reconstruction takes place at delayed times.

We stated above that the dispersion relation of the bulk dynamic medium is a band structure which exhibits forbidden wavevector bandgaps. This dispersion relation yields infinite group velocities at frequencies $\omega_c=\Omega m/2$ with integer m. This frequency condition is satisfied in Fig. 1 and Table 1 with $\omega_c=\Omega/2$. However, as can be seen in the Table 1, the peak velocities do not diverge, that is, the time delay $\Delta\tilde{\tau}_n$ is finite for all the partial pulses n. This is not really surprising, given the fact that the group velocity in the bulk medium is in general different than the peak velocity (velocities) of a pulse (pulses) emerging from a slab of the same medium. In fact, the group and peak velocities could coincide only if the incident pulse does not decompose into several pulses in the medium (which is the case in Refs. [1, 2]). However, clearly, that is not the case at hand, for, inside our dynamic slab there is, in principle, an infinite number of partial pulses centered at $\omega_c-n\Omega$ and moving to the left and right.

4. Gaussian pulses with large spectral band-widths

Now we discuss the transmission of a Gaussian pulse with a large spectral bandwidth ($\Delta\omega/\Omega>1$) which corresponds to a short pulse. Since the outcoming pulse is the result of the superposition of a large number of harmonics that are created in the slab by the extended range of frequencies of the incident pulse, the analysis of the transmission of these pulses passing through the dynamic slab is complicated. We consider an incident Gaussian pulse with carrier frequency $\omega_c/\Omega=5$ and bandwidth $\Delta\omega/\Omega=5$ as depicted in Fig. 4(a). The transmitted pulses with the slab modulated at strengths $M=0.162$ (moderate modulation) and $M=0.648$ (strong modulation) and for normalized modulation frequency $\tilde{\Omega}=2$ and 8 are also illustrated in Fig. 4. Interestingly, for the behavior in time we observe that after the main pulse traverses the slab (with peak at $\tilde{t}\approx 1$), two small pulses emerge. For the moderate modulation and both normalized modulation frequencies, these pulses are peaked at $\tilde{t}\approx 3$ and $\tilde{t}\approx 5$. From Eq. (23), we recall that $\tilde{t}\approx 1$ is just the normalized time for light propagating at the speed $v_s=c/\sqrt{\varepsilon}$ to traverse the slab. Such behavior could be expected for a transparent *static* plate, provided that the temporal width $\tau=2/\Delta\omega$ of the pulse is much smaller than the transit time D/v_s (a condition satisfied in Fig. 4). Under such circumstances, because of Fabry-Perot reflections, a series of pulses should emerge with their peaks exiting the slab at the times $D/v_s, 3D/v_s, 5D/v_s,\ldots$ (normalized times $\tilde{t}=1,3,5,\ldots$). Thus, it is not all that surprising that, for $\tau\ll D/v_s$ and moderate modulation, several of these transmission peaks are found. (On the contrary, if $\tau\gg D/v_s$, as occurs for the quasi-monochromatic case, then the emerging wave forms strongly overlap and a single pulse is observed, see Figs. 1-3. Evidently, the physics at hand is very different). However, in our dynamic slab, an infinite number of plane waves p and harmonics n interfere, so it is rather unexpected that the exit times $\tilde{t}=2.98$ and 5.05 for $\tilde{\Omega}=2$ and $\tilde{t}=2.99$ and 4.99 for $\tilde{\Omega}=8$ (for the moderate modulation) are so near to $\tilde{t}=3$ and 5 of the static plate. On the other hand, in the case of strong modulation ($M=0.648$), greater departure from these times is experienced [see Fig. 4(b)]. Also, the emergent peaks at $\tilde{t}\simeq 3$ are considerably diminished in comparison to the primary peak at $\tilde{t}\simeq 1$, and the peaks at $\tilde{t}\simeq 5$ can be scarcely seen on the scale of Fig. 4. As a final comment, for strong modulation we can observe considerable distortion in the wings of the transmitted pulse, obviously due to the generation of significant high-order harmonics.

#159929 - $15.00 USD Received 14 Dec 2011; revised 19 Jan 2012; accepted 26 Jan 2012; published 22 Feb 2012

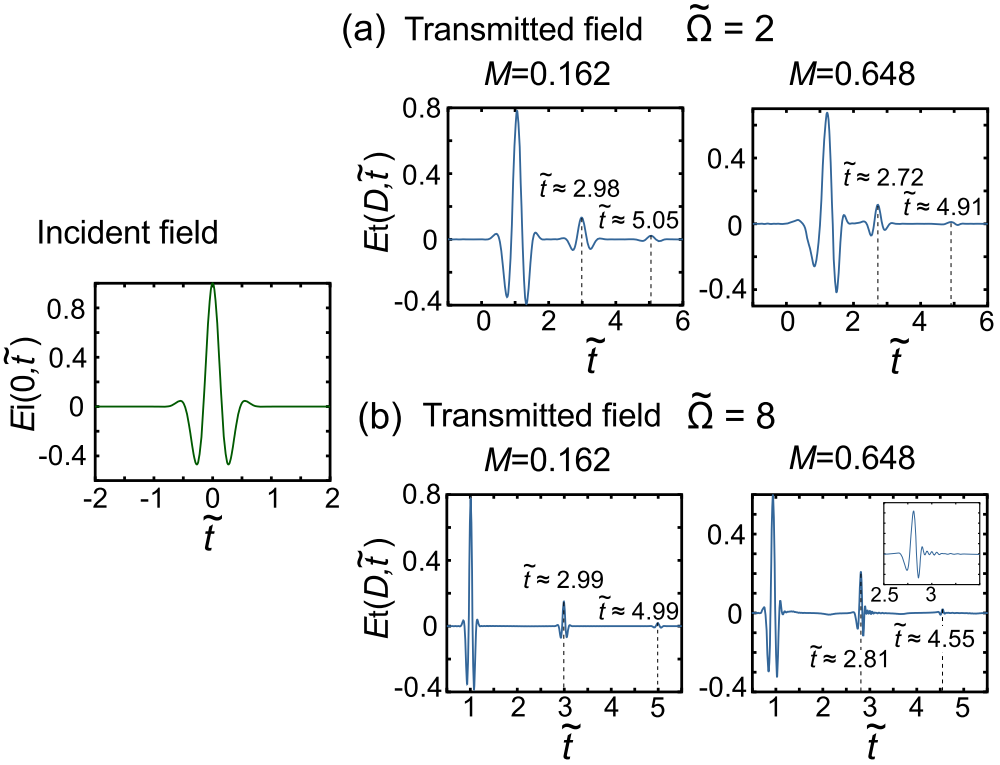

Fig. 4. Incident and transmitted pulses vs. the normalized time $\tilde{t}$ for $M = 0.162$ (moderate modulation) and $M = 0.648$ (strong modulation). The incident Gaussian pulse has a large bandwidth $\Delta\omega/\Omega = 5$ and carrier frequency $\omega_c/\Omega = 5$, and the normalized time $\tilde{t}$ is taken with respect to $\tilde{\Omega} = 2$. (a) $\tilde{\Omega} = 2$ and $t_s\Delta\omega = 10$. (b) $\tilde{\Omega} = 8$ and $t_s\Delta\omega = 40$ (the inset is a closeup of the second pulse). Here $\omega_c\tau = 2$.

5. Peak velocity

According to our result Eq. (17), every harmonic component of frequency $\omega - n\Omega$ exits the slab with the very same envelope form as the quasi-monochromatic incident pulse. Then, for a Gaussian pulse incident at the slab, all the emerging partial pulses are also Gaussian. What can we say about the superposition of these pulses, namely, the total electric field $E_t(y = D,t)$, as given by Eq. (17)? In general one cannot expect that all these partial pulses will coalesce into a single pulse. However, this *does* occur for pulses that are wide in time, $\omega_c\tau \gg 1$, and Figs. 1-3 confirm that, indeed, for $\omega_c\tau \simeq 10$ a single well defined pulse exits the slab. The peak velocity of such a pulse is a measurable quantity, and it is worthwhile examining its dependence on the parameters that define the dynamic-periodic slab and the pulse itself.

In what follows, we analyze the peak velocity v_p of a Gaussian pulse with small spectral width ($\Delta\omega/\Omega = 0.1$ and 0.01) and carrier frequency $\omega_c/\Omega = 0.5$ for which the group velocity is infinite, as seen in the inset of Fig. 5. This velocity is determined from the transit time of the peak of the pulse, namely, we calculate the transmitted electric field as a function of time at $y = D$ and observe the time t_o that it takes for the peak of the Gaussian pulse to traverse the slab of width D. The velocity is obtained from $v_p = D/t_o$. In Fig. 5 we plot the peak velocity v_p normalized to the velocity v_s as a function of the normalized thickness $(\Omega\sqrt{\varepsilon}/c)D$. The cases compared are no modulation ($M = 0$), weak modulation ($M = 0.016$) for $\Delta\omega/\Omega = 0.1$,

#159929 - $15.00 USD Received 14 Dec 2011; revised 19 Jan 2012; accepted 26 Jan 2012; published 22 Feb 2012

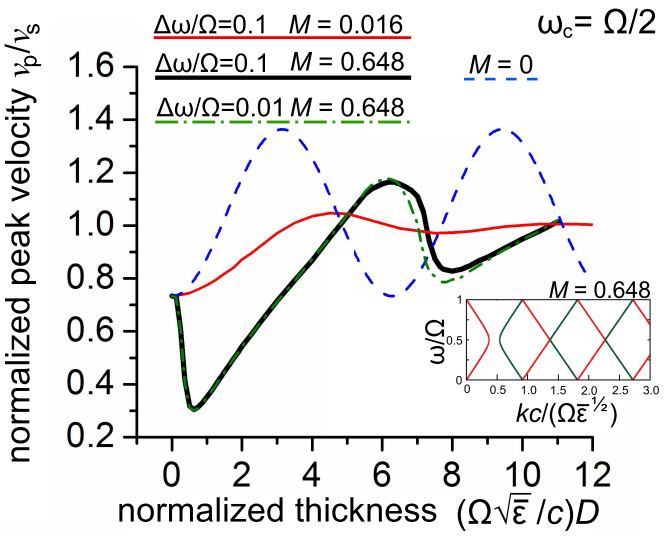

Fig. 5. Peak velocity of a Gaussian pulse with carrier frequency $\omega_c/\Omega = 0.5$, as a function of the normalized thickness $(\Omega\sqrt{\bar{\varepsilon}}/c)D$ for weak ($M = 0.016$) and strong ($M = 0.648$) modulations with $\Delta\omega/\Omega = 0.1$, strong modulation with reduced spectral width $\Delta\omega/\Omega = 0.1$, and a *static case*. For the static case $M = 0$ we consider a wide pulse in time with $\tau \gg D/v_s$. The inset is the bulk dispersion relation [normalized frequency ω/Ω vs. normalized wavevector $kc/(\Omega\sqrt{\bar{\varepsilon}})$] for the strong modulation as in Ref. [12].

and strong modulations ($M = 0.648$) for $\Delta\omega/\Omega = 0.1$ and 0.01. The velocity of the peak in the absence of modulation is obtained from Ref. [26], which deals with the peak velocity for a wide Gaussian pulse ($\tau \gg D/v_s$ in addition to $\omega_c\tau \gg 1$), interacting with a static plate in vacuum. In Ref. [26], the following peak velocity has been derived:

$$v_p = v_s\left[\frac{2\sqrt{\bar{\varepsilon}}}{1+\bar{\varepsilon}}\cos^2\left(\omega_c\sqrt{\bar{\varepsilon}}D/c\right) + \frac{1+\bar{\varepsilon}}{2\sqrt{\bar{\varepsilon}}}\sin^2\left(\omega_c\sqrt{\bar{\varepsilon}}D/c\right)\right]. \tag{25}$$

Equation (25) is plotted for comparison with the dynamic plate. For $\Delta\omega/\Omega = 0.1$ and $(\Omega\sqrt{\bar{\varepsilon}}/c)D \ll 1$, the peak velocity v_p in absence of modulation is seen to converge to that obtained for the weak modulation strength. Indeed, Fig. 5 confirms that, in the limit $D \to 0$, all four curves converge to $v_p/v_s = 2\sqrt{\bar{\varepsilon}}/(1+\bar{\varepsilon}) = 0.733$, obtained from Eq. (25).

It is apparent from Fig. 5 that the slab width is an important factor in the resulting peak velocity. We observe that the transit time is not proportional to the slab width; as the slab thickness increases, the velocity of the pulse may rise or fall. Results in Fig. 5 indicate *an oscillatory behavior of the velocity of the peak with the thickness of the slab*. This behavior is *in part* associated with interference, in the dynamic slab, of all the harmonics $\omega - n\Omega$, and the infinite number of plane waves with wave vectors $k_p(\omega)$ for each of these frequencies. However, even in the absence of modulation, for a pulse with $\tau \gg D/v_s$ [see Fig. 5 and Eq. (25)], the peak velocity is a periodic function of the slab thickness D, with period $\lambda/2$, where $\lambda = 2\pi c/(\omega_c\sqrt{\bar{\varepsilon}})$ is the wavelength in the plate. A generalization of Eq. (25) to allow for absorption (see Ref. [27]) also shows that the peak velocity varies with the thickness although is no longer a periodic function of D. Now, expressing the peak velocity (25) in terms of $(\Omega\sqrt{\bar{\varepsilon}}/c)D$ [using Eq. (22)] results in the period of 2π. It is interesting to observe that, for weak modulation ($M = 0.016$), an approximate spacing of 2π between minima can be indeed noticed, despite the fact that in this case the pulse is not very wide in time. Nevertheless, the shape and amplitude of the

#159929 - $15.00 USD Received 14 Dec 2011; revised 19 Jan 2012; accepted 26 Jan 2012; published 22 Feb 2012

oscillations for the weak modulation and for lack of modulation (with a very wide pulse) differ substantially for most of the $(\Omega\sqrt{\varepsilon}/c)D$ range.

For the dynamic cases [see Fig. 5], the behavior is more complicated than it is for static conditions. The interference of all waves generated in the medium results in differing peak velocities for different thicknesses. As the modulation increases, the velocity profile changes and the separation between minima deviates from 2π. For strong modulation it is not possible to extend the analysis to very large slab widths due to the increased deformation of the transmitted pulse.

As it has been seen, the peak velocity $v_{\rm p}$ is sensitive to the modulation strength M. This was expected since the dispersion relation changes with the modulation strength (see Fig. 3 in Ref. [12]), thus affecting the speeds of the frequency components of the pulse. Also, from Fig. 5, the peak velocity $v_{\rm p}$ depends on the spectral width of the pulse (see strong modulation for $\Delta\omega/\Omega = 0.1$ and 0.01). Despite the bandwidths $\Delta\omega/\Omega$ here differing by an order of magnitude, the peak velocities $v_{\rm p}$ for these cases are nearly equal. In fact, if we reduced the spectral width by one more order of magnitude we would observe, on the scale of Fig. 5, that the corresponding peak velocity plot would overlap with that for $\Delta\omega/\Omega = 0.01$. Thus, for this case, the velocity is not sensitive to the spectral width of the pulse.

We have also calculated the peak velocity $v_{\rm p}$ as a function of the modulation strength M (with $(\Omega\sqrt{\varepsilon}/c)D$ and $\Delta\omega/\Omega$ as parameters) and as function of the normalized bandwidth $\Delta\omega/\Omega$ (with $(\Omega\sqrt{\varepsilon}/c)D$ and M as parameters). The most important conclusion from this analysis, as well as from Fig. 5 is that, for an incident Gaussian pulse and sinusoidal variation in time of the dielectric function, *the infinite group velocities* found in Ref. [12] at integer multiples of half the modulation frequency ($\omega = \Omega n/2$ with n an integer) have no repercussions for the peak velocity $v_{\rm p}$ of the transmitted pulse. This is due to the slab boundaries and the broadening of the transmitted pulse spectral content (generation of harmonics by the dynamic slab) which void the description based on a single pulse that traverses the slab at the group velocity in the bulk medium (see Sec. 3). Moreover, while the peak of the pulse can travel at speeds above $v_{\rm s} = c/\sqrt{\varepsilon}$, the pulse peak velocity $v_{\rm p}$ is never superluminal (contrary to the case of Table 1 for $\omega_{\rm c} = \Omega/2$ where the partial peak velocity for $n = -2$ is $v_{-2} = 1.7c$), at least for our closely studied carrier frequency $\omega_{\rm c} = \Omega/2$.

6. Energy considerations

Ordinarily, for a transparent material, it is expected that the incoming energy breaks down exactly into the reflected and transmitted energies. However, since our system involves an unspecified external agent modulating the dielectric function, this is an open system that may result in supplying energy to the medium. Hence, conservation of energy is not necessarily satisfied. This issue was discussed previously for response of a dynamic-periodic slab to monochromatic incidence, even resulting in huge, resonant amplification of an incident plane wave [12, 13]. Herein we extend that study to an incident pulse. We define the reflectance $\mathscr{R}$ (transmittance $\mathscr{T}$) as

$$\mathscr{R}(\mathscr{T}) = \int_{-\infty}^{\infty} |A_{\rm r(t)}(\omega)|^2 {\rm d}\omega \Big/ \int_{-\infty}^{\infty} |E_{\rm o}(\omega)|^2 {\rm d}\omega. \tag{26}$$

Here $A_{\rm r}(\omega)$ [$A_{\rm t}(\omega)$] is the Fourier transform of the reflected [transmitted] field $E_{\rm r}(0,t)$ [$E_{\rm t}(D,t)$] at the entrance [exit] interface. By applying the variable transformation $\omega \to \omega + n\Omega$ to Eqs. (6,7), it follows that

$$A_{\rm r}(\omega) = \sum_{n=-\infty}^{\infty} r_n(\omega + n\Omega) E_{\rm o}(\omega + n\Omega), \quad A_{\rm t}(\omega) = \sum_{n=-\infty}^{\infty} t_n(\omega + n\Omega) E_{\rm o}(\omega + n\Omega). \tag{27}$$

#159929 - $15.00 USD Received 14 Dec 2011; revised 19 Jan 2012; accepted 26 Jan 2012; published 22 Feb 2012

In Table 3, we have computed the sum of the reflectance and transmittance ($\mathscr{R}+\mathscr{T}$), using Eqs. (26) and (27), under a variety of conditions. Table 3 indicates that the sum of the reflected

Table 3. Sum of the reflectance and transmittance ($\mathscr{R}+\mathscr{T}$) for incident Gaussian pulses with carrier frequency $\omega_c/\Omega = 0.5$ and 1 and spectral width $\Delta\omega/\Omega = 0.1$; a normalized modulation frequency $\tilde{\Omega} = 2$, and modulation strengths $M = 0.016$ (weak), 0.162 (moderate), and 0.648 (strong).

ω_c/Ω	M	$\mathscr{R}+\mathscr{T}$
0.5	0.016	1.002
	0.162	1.033
	0.648	1.276
1	0.016	1.000
	0.162	1.007
	0.648	1.151

and transmitted energies exceeds the energy of the incident pulse ($\mathscr{R}+\mathscr{T} > 1$) with the exception of the case $\omega_c/\Omega = 1$ and $M = 0.016$ in which the gained energy is practically zero. Obviously, this energy excess is supplied by the external agent. Also, we notice from Table 3 that as the modulation is increased, more energy is provided by the external modulating agent.

We have shown, as expected from our previous studies [12, 13], that pulses traversing a dynamic-periodic slab can gain energy that is delivered by the external modulating agent.

7. Conclusions

We presented a theory of pulse propagation through a slab whose dielectric function varies periodically with time. This theory follows from our previous work limited to monochromatic excitation [12].

For quasi-monochromatic pulses, we found that the transmitted pulse at the exit surface can be decomposed as a superposition of pulses. This representation is derived from the concepts of phase and group delays and the outcoming pulse is completely characterized by the monochromatic transmission coefficients $t_n(\omega_c)$ of the harmonics n generated by the carrier frequency ω_c. The carrier signals of these partial pulses have frequencies $\omega_c - n\Omega$ and acquire phase shifts $\phi_n(\omega_c)$, and these pulses exit the slab with the same form of their envelope as the incident pulse and with temporal shifts $\phi_n'(\omega_c)$. In this sense then, no distortion occurs in the pulse shape. We analyzed the case of an incident monochromatic Gaussian pulse for several normalized modulation frequencies, carrier frequencies, and modulations strengths. We showed that the peak velocity of the partial pulses can be both fast ($v_n > c$ or $v_n < 0$) or slow ($v_n \ll c$). It turns out that infinite group velocities occurring in the band structure at frequencies $\omega = \Omega m/2$ (m is an integer) are not related to any of the partial peak velocities v_n. In the other extreme of very short pulses, we studied the transmitted pulses for an incident Gaussian pulse with a large bandwidth for several modulation frequencies and modulation strengths. Since here $\tau \ll D/v_s$, we obtained multiple pulses coming out of the slab at different times t due to the multiple round trips of the pulse between the slab surfaces. As a consequence, the amplitude of each pulse successively decreases upon each round. We found that these pulses exit the slab with delay times $\tilde{t} \approx 1, 3, 5, \ldots$ (the equality would give the exact pulse exit times for an unmodulated slab). The departure from these times is larger as the modulation strength increases. Also, in this case the pulses become more distorted.

We also investigated the peak velocity v_p of the transmitted pulse when $\tau \gg D/v_s$ and $\omega_c\tau \gg 1$, that is, when a single well defined pulse exits the slab. We found that the peak ve-

#159929 - $15.00 USD Received 14 Dec 2011; revised 19 Jan 2012; accepted 26 Jan 2012; published 22 Feb 2012

locity v_p follows an oscillatory behavior as a function of the normalized thickness $(\Omega\sqrt{\bar{\varepsilon}}/c)D$ (similar to the unmodulated case). This behavior depends strongly on the modulation strength M and weakly on the incident pulse spectral width $\Delta\omega/\omega_c$. The peak velocity v_p turned out be faster or slower than v_s, but never faster than c for the analyzed cases. In these cases, the carrier frequency was $\omega_c = \Omega/2$ for which the bulk dispersion relation renders an infinite group velocity. We concluded that this divergence has no repercussions for the transmitted pulse peak velocity v_p. At last, we mention that a strong modulation strength M and a large slab thickness can lead to strong pulse deformation.

Further, we performed numerical calculations of the reflected and transmitted energies for an incident Gaussian pulse with particular parameters. We showed that, in general, the sum of these energies can exceed the incident energy. This gained energy is supplied by the external modulating agent.

Current and future developments could lead to the implementation of metamaterials that can be strongly and rapidly modulated and operated at higher frequencies than microwaves. Then, hopefully, our dynamic-periodic slab could be applied as a controlling device for the propagation velocity of light pulses. Also, such a dynamic slab could be used as a generator of pulses with up-conversion of the carrier frequency.

Acknowledgments

J. H. A.-P. thanks CONACyT for support through the scholarship 212472. P. H. is grateful to Tomás López-Ríos for his hospitality at CNRS Grenoble during a sabbatical year. He also acknowledges support through the CONACyT projects 79180 and 103644-F.

#159929 - $15.00 USD Received 14 Dec 2011; revised 19 Jan 2012; accepted 26 Jan 2012; published 22 Feb 2012